東北大学機関リポジトリ
TOUR
Tohoku University Repository
東北大学

Formation and Mechanical Strengths of Aluminum-based Supersaturated Solid Solutions((A)Amorphous Alloys)

著者	Inoue Akihisa, Watanabe Mitsuru, Kimura Hisamichi, Masumoto Tsuyoshi
journal or publication title	Science reports of the Research Institutes, Tohoku University. Ser. A, Physics, chemistry and metallurgy
volume	36
number	1
page range	59-77
year	1991-03-25
URL	http://hdl.handle.net/10097/28366

Formation and Mechanical Strengths of Aluminum-based Supersaturated Solid Solutions*

Akihisa Inoue, Mitsuru Watanabe+, Hisamichi Kimura and Tsuyoshi Masumoto

Institute for Materials Research

(Received December 28, 1990)

Synopsis

This paper deals with the recent data on the formation ranges, microstructure and mechanical properties of nonequilibrium supersaturated solid solution including fcc and amorphous phases in Al-Ln-TM (Ln=lanthanide metal, TM=transition metal) ternary system produced by rapid solidification. The tensile fracture strength (σ_f) increases with increasing solute elements and the highest σ_f is about 860 MPa for the fcc supersaturated solution and 1280 MPa for the amorphous phase. The compositional dependence of σ_f for both phases is dominated by the bonding nature among the constituent elements and independent of their atomic size ratios and atomic arrangements.

I. Introduction

The solid solution-strengthening method resulting from the formation of a supersaturated solid solution containing solute elements above their equilibrium solubility limit is known as one of the strengthening methods of metallic materials. By utilizing the extension of the solid solubility limit caused by water quenching from a solid solution region at high temperatures, a number of high-strength metallic materials have been developed up to date. The rapid solidification method from a liquidus state is expected to bring about a further extension of solubility limit for solute elements as compared with the

---

* The 1869th report of Institute for Materials Research.

+ Department of Metallurgy, Mining College, Akita University, Akita 010.

compared with the water quenching technique in a solidus state. Klement et al.[1] applied the rapid quenching technique to a Au-Si system with the aim of obtaining a solid solution with an extended solubility limit and succeeded in producing an amorphous Au-Si phase in 1960. The amorphous phase can be regarded to be a kind of solid solution which has a favorable atomic arrangement so as to reduce a strain resulting from the supersaturated dissolution of solute elements and hence is an ideal supersaturated solution with a homogeneous distribution of constituent elements and an isotropic atomic arrangement.

Since the formation of the amorphous Au-Si phase, a great number of studies on the formation of Al-based supersaturated solutions by liquid quenching have been carried out[2,3] from scientific and engineering points of view. If we can produce an amorphous phase containing a large amount of solute elements in Al-based alloy systems, there is a high possibility that a new Al-based material with extremely high mechanical strengths is developed. This paper is intended to review our recent data on the formation and mechanical strengths of Al-based supersaturated solutions with an fcc or an amorphous structure produced by rapid solidification.

One can list up various rapid solidification techniques of gun, piston-anvil, single-roller melt spinning, twin roller, atomization by use of coolents of gas, water and oil, and in-rotating-water liquid quenching etc.[4] The cooling velocity from the melt is strongly dependent on their quenching techniques, resulting in a significant difference in the phase fields where their supersaturated solutions are formed. This paper focusses on the data on Al-based alloys produced by the single-roller melt spinning technique which yields a relatively uniform cooling rate over the whole sample and enables us to have mass production.

II. Dominant Parameters for the Extension of Solubility Limit

Little has been obtained about systematic information on the maximum solid solubility of solute elements into an fcc Al phase for melt-spun Al-based alloys. Accordingly, the maximum solubility limit of solute elements into an Al phase in Al-based binary alloys obtained by the piston-anvil and gun methods is summarized in Table 1, along with the equilibrium solubility limit and eutectic or peritectic compositions[3,5]. The solubility limit of the rapidly solidified alloys can be divided into the following three types;

Table 1 Maximum solubility of solute elements in Al-based binary alloys in equilibrium and rapidly solidified states[3,5]. (at%)

Solute	Equilibrium		Maximum extended solubility
	Maximum solubility	C_e or C_p	
Eutectic			
Ag	23.8	37.0	25-40
Mg	16.3	36.4	36.8-40
Cu	2.5	17.5	17-18
Si	1.6	12.0	10-16
Mn	0.9	0.95	6-10
Fe	≅0.02	0.9	4-6
Co	<0.01	0.45	0.5-5
Ni	≅0.02	2.8	1.2-7.7
Ce	0.01	2.6	1.9
Peritectic			
Ti	0.6	0.06	0.2-2
Cr	0.4	0.19	5-7
V	0.25	0.05	1.4-2
Zr	0.09	0.03	1.2-1.5
Mo	0.07	0.03	1.0-1.5
W	0.02	0.01	0.9-1.9

C_e=eutectic composition, C_p=peritectic composition.

(1) Ag and Mg with the solubility range above 20 at%,

(2) Cu, Si, Mn, Cr, Ni, Fe and Co with the solubility range of 3 to 20 at%, and

(3) Ce, Ti, V, Zr, Mo and W with the solubility range less than 3 at%.

The difference among their solubility ranges is closely related to the maximum solubility limit in an equilibrium state and the eutectic and peritectic compositions. As shown in Table 1, the solute elements with a eutectic-type equilibrium phase diagram have a wider solubility range as compared with those with a peritectic-type equilibrium phase diagram. Figure 1 shows the relation between the maximum solubility limit obtained by liquid quenching shown in Table 1 and the atomic size ratio of M elements to Al. It is noticed that the maximum solubility limit of Mo and W is very small, in spite of their small atomic size ratios. One cannot see a general tendency that the solubility limit increases with a decrease of the atomic size ratio, suggesting that the extension of the solubility limit of M elements into Al phase is dominated by other factors except the atomic size ratio.

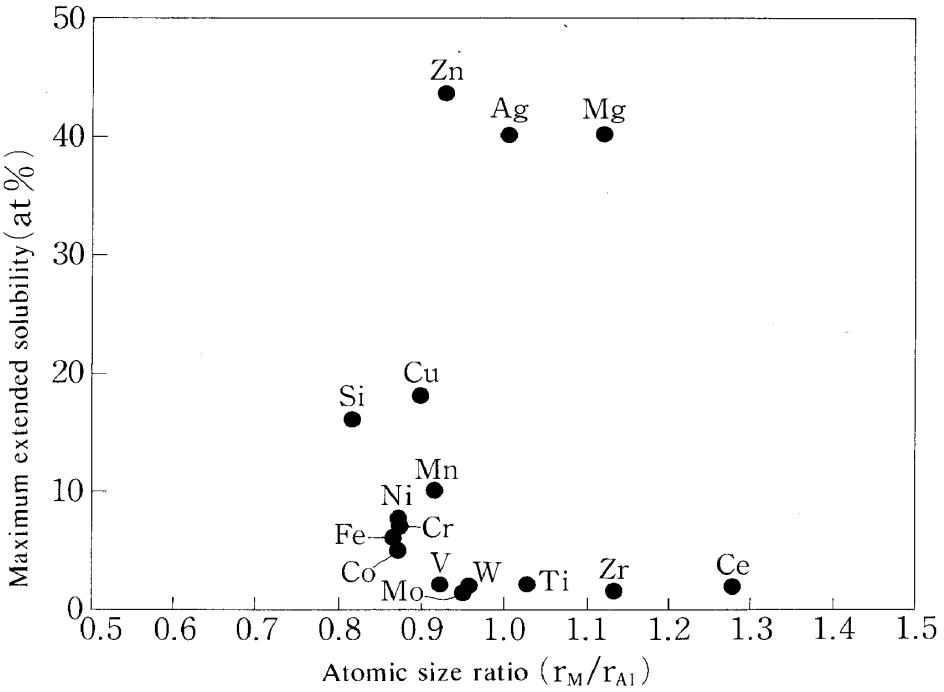

Fig. 1 The relation between maximumly extended solubility limit of solute elements (M) into fcc Al phase for liquid-quenched Al-M binary alloys and the atomic radius ratio of M to Al.

Even by use of the single-roller melt spinning method with a cooling rate lower than that for the piston-anvil and gun methods, an fcc supersaturated solution has been found[6] to form in the M range less than 5 at% for all $Al_{95-x}M_xSi_5$ (M=Ti, Zr, Hf, V, Nb, Cr, Mo, Mn, Fe, Co, Ni or Cu) alloys containing 5 at% Si. It has been interpreted that the supercooling capacity of the Al-based alloys is enhanced by the addition of 5 at% Si, leading to an extension of the solid solubility limit. The high-strength alloys caused by the formation of supersaturated solid solution consist usually of multicomponents containing more than three elements. Consequently, in addition to the information on the solubility limit of M elements into Al phase in the Al-M binary alloys produced by the piston-anvil and gun methods shown in Table 1, accummulation of systematic research data on the change of supercooling capacity of Al-based alloys by multiplication of alloy components is required to develop high-strength Al-based alloys by utilizing the solid-solution strengthening.

Most recently, we have found that an amorphous single phase forms in the Ln range of 7 to 13 at% in Al-Ln binary system[7-9] and the glass formation range is extended up to the Ln+M content of about 30 at% in Al-Ln-M ternary system[10,11]. As shown in the X-ray

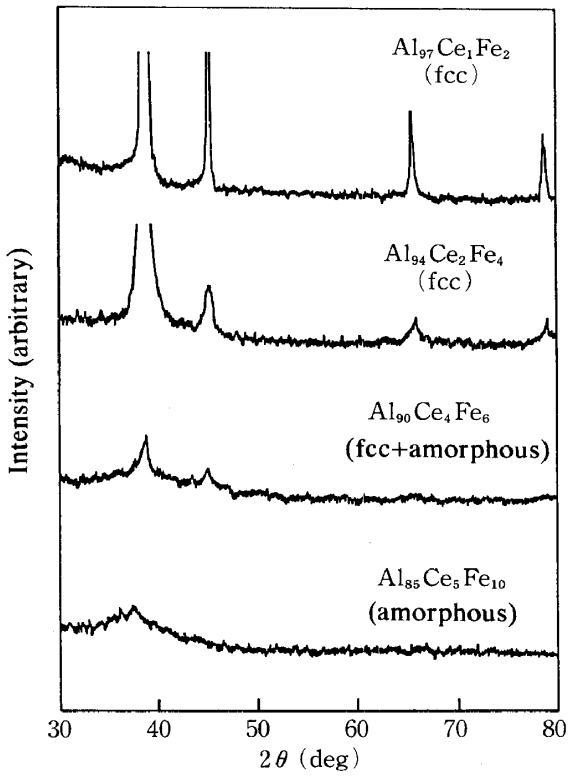

Fig. 2 X-ray diffraction patterns showing the structural change from fcc-Al to amorphous phase for melt-spun Al-Ce-Fe ternary alloys.

the X-ray diffraction patterns of Al-Ce-Fe ternary alloys in Fig. 2, an fcc supersaturated solution forms at the concentration side lower than the glass-formation range. Accordingly, the finding of the glass-formation range in Al-based alloys implies a remarkable extension of the formation range of the supersaturated solution. As a typical example for the ternary system, the phase field in rapidly solidified Al-Ce-Fe alloys is shown in Fig. 3[12]. The fcc solution and the amorphous phase form in each range below about 3 at% Ce and 6 at% Fe and above about 2 at% Ce and 5 at% Fe and the coexistent fcc and amorphous phases form in the intermediate range, indicating clearly that the solubility limit is remarkably extended by multiplication to the ternary system.

The atomic volume ratio of Ln to Al is as large as 1.80 to 2.50, while that of the transition metals such as Cr, Mn, Fe and Co etc. which do not cause the formation of amorphous and fcc phases is as small as 0.65 to 0.72. It is thus said that the atomic size ratio is much larger for the Ln elements leading to the formation of the supersaturated solution in much wider composition ranges. These data allow us to interpret that the atomic size ratio is not a dominant factor for the formation of the supersaturated solution, in agreement

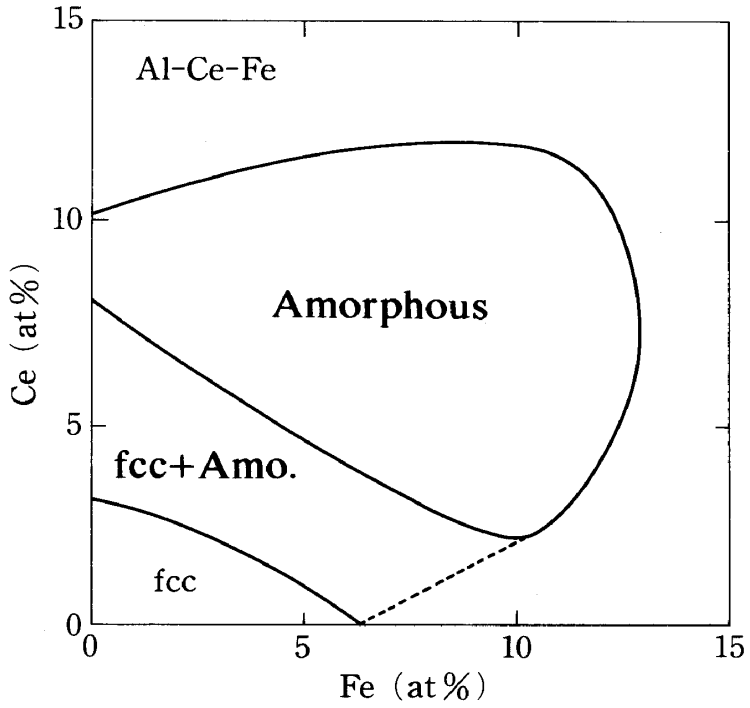

Fig. 3 Phase field of melt-spun Al-Ce-Fe ternary alloys.

with the result described in Fig. 1. The interpretation based on the enhancement of supercooling capacity of alloy liquids and the degradation of nucleation and growth of compounds seems to be important for clarification of the mechanism for the formation of the supersaturated solution over a wide composition range.

III. Effect of Solute Elements on the Mechanical Strengths of fcc Supersaturated Solutions

Figure 4 shows the changes in the tensile fracture strength (σ_f) and Vickers hardness (H_v) of fcc $Al_{92}M_3Si_5$ solutions produced by rapid solidification with M elements[6]. The grain size of the fcc solutions is in the range of 0.5 to 1.5 μm and almost independent of the M elements. On the other hand, the σ_f and H_v change systematically with atomic number of the M elements and have maximum values around Mn and Fe. These changes cannot be explained only by the atomic size ratio of the M elements to Al and indicate the necessity of taking the bonding nature between Al and M atoms based on the outer electron concentration into consideration. That is, the strength of the fcc

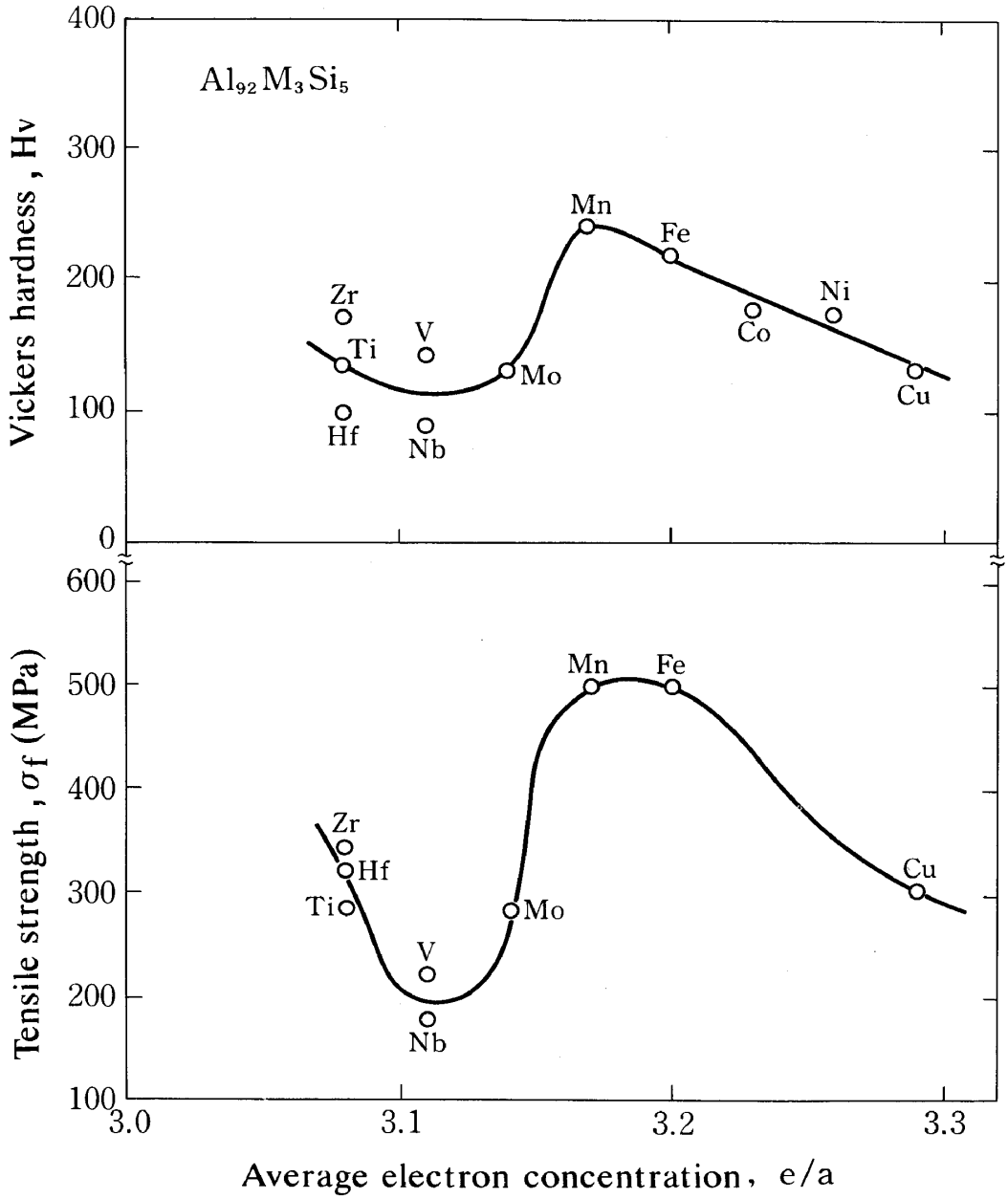

Fig. 4 Changes in the tensile fracture strength (σ_f) and Vickers hardness (H_v) as a function of outer electron concentration (e/a) for fcc $Al_{92}M_3Si_5$ solutions produced by melt spinning.

solution is not dominated by the solid solution strengthening resulting from the atomic size ratio but by the bonding nature between the sp electrons in Al and the 3d electrons in the M elements. A half in the 3d electron shell for Mn and Fe elements is filled and the

electronic state brings about a confirm bonding between Al and M atoms, leading to the achievement of high mechanical strengths. The refinement of grain size and the introduction of extra lattice defects obtained by rapid solidification are important factors for the achievement of high mechanical strengths for the rapidly solidified alloys as compared with those for the conventionally solidified alloys. In order to enhance further the mechanical strengths of the rapidly solidified alloys, one can recognize the importance of the alloy design leading to an electronic state in the outer shell so as to cause a large attractive bonding interaction among the constituent elements.

The mechanical strengths of the fcc solution in Al-Fe-Si and Al-Mn-Si systems remain constant, even though the Si content increases significantly. Considering the result that no compound is formed in Al-Si system, the nearly constant strengths are presumably because Si has a repulsive interaction against Al and a strong bonding state does not occur in the Al-Si atomic pair, in agreement with the present experimental results.

IV. High-Strength fcc Solutions

On the basis of the concept described in section 3, we can predict an alloy system in which the fcc solution with high mechanical strengths is obtained. As an example, one can notice an Al-Ce-Fe system. As shown in Fig. 4, the dissolution of an Fe element is the most effective for the increase in H_v and σ_f presumably because of the large negative bonding nature against Al and Ce elements. In addition, the melting temperature (T_m) of Al-Ce intermetallic compounds is relatively high in a large number of Al-based binary compounds and there is no appreciable solubility of Ce into Al phase in an equilibrium state because of the large atomic size ratio between Ce and Al atoms. Figure 5 shows the compositional dependences of H_v and σ_f for the fcc solution in Al-Ce-Fe system[6]. It is notable that the H_v and σ_f reach 440 and 860 MPa for $Al_{95}Ce_1Fe_4$. These strengths are higher than the highest values[13] for the fcc solution with good ductility reported up to date, indicating an appropriateness of the alloy design based on the above-described concept. The fcc phase consists of equiaxed grains with a grain size of about 0.3 μm and contains an extremely high density of dislocations, as shown in Fig. 6. The introduction of such a high density of dislocations is not obtained in an as-quenched state in the Al-M binary alloys and is

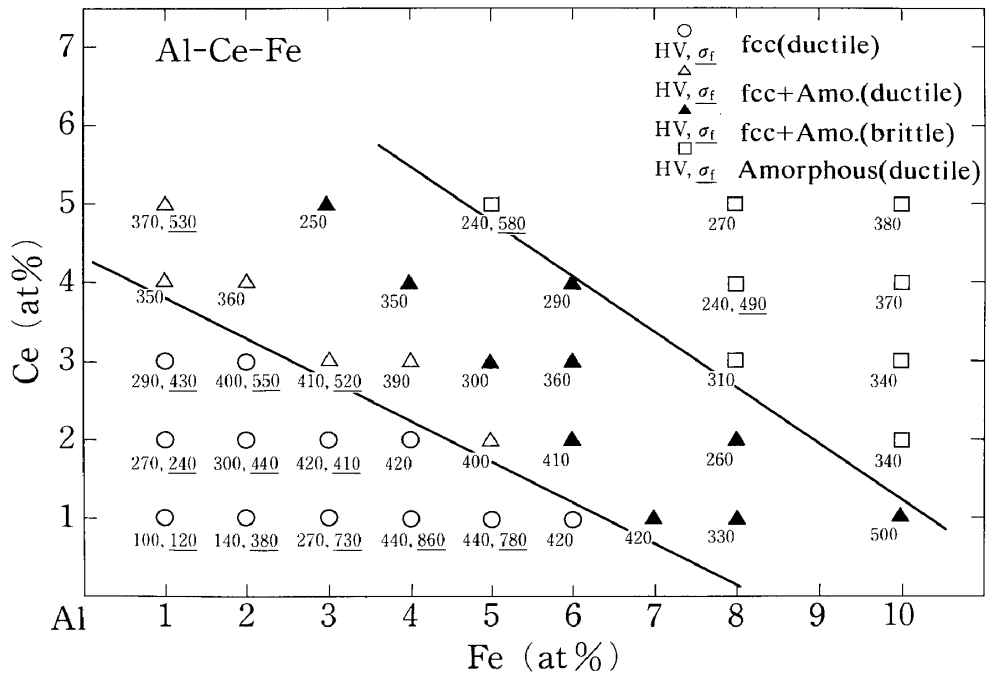

Fig. 5 Compositional dependences of tensile fracture strength (σ_f) and Vickers hardness (H_v) of fcc and amorphous phases in melt-spun Al-Ce-Fe alloys.

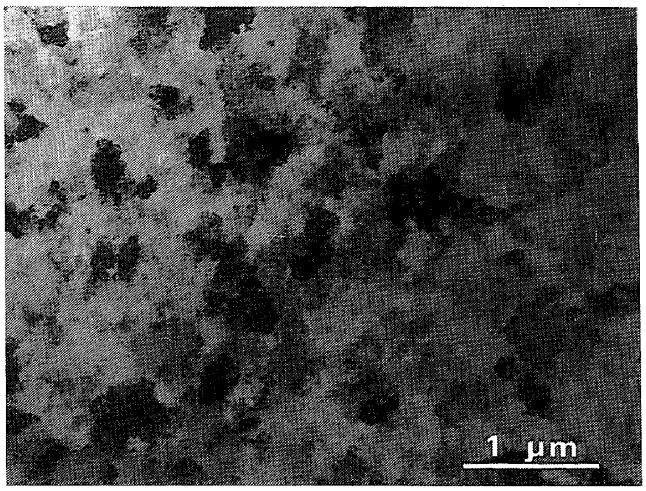

Fig. 6 Bright-field electron micrograph of a melt-spun $Al_{95}Ce_1Fe_4$ alloy.

presumably due to the increase of supercooling capacity of alloys by the multiplication of alloy components into the ternary system. Thus, the reason for the achievement of high mechanical strengths for the Al-Ce-Fe fcc solution is presumably due to the introduction of a high density of internal defects resulting from the increase of supercooling capacity as well as the strong bonding nature among the constituent elements. In addition to the fcc solution in Al-Ce-Fe system, a similar fcc solution containing a high density of dislocations is formed in Al-Y-Fe system by rapid solidification and the high strengths of 355 for H_v and 705 MPa for σ_f are obtained for $Al_{95}Y_1Fe_4$[14].

V. Formation and High Mechanical Strengths of Amorphous Alloys

As described in section 2, the Al-based amorphous alloys in which solute elements above the equilibrium solubility limit are dissolved and a periodic atomic arrangement does not exist on a long-range scale can be formed through the increase in the supercooling capacity resulting from an appropriate combination of alloy elements and the suppression of nucleation and growth of a crystalline phase. The appearance of the amorphous phase enables us to dissolve a large amount of solute elements above the maximum solubility limit for the crystalline supersaturated solution, leading to an increase of strength and toughness. The Al-based alloys with high strengths and high toughness by taking advantage of amorphization of alloys were produced for the first time in 1987[15]. In this section, we describe the formation and mechanical strengths of Al-based amorphous alloys from the standpoint of a kind of supersaturated solid solution.

The alloy components of Al-based amorphous alloys containing more than 75 at% Al can be divided into two categories of metal-metalloid and metal-metal types[16]. The former type consists of Al-M-Si, Al-M-Ge and Al-M-B systems where M is V, Nb, Mo, Mn, Fe, Co, Ni or Cu. As an example, the composition range in which an amorphous phase in the Al-M-Si system is formed by rapid solidification is shown in Fig. 7[17]. The amorphous phase is formed in very wide composition ranges of 12 to 43 at% Si and 5 to 23 at% M. However, the formation of ductile amorphous alloys which can be bent though 180 degrees is limited to the range above about 80 at% Al in Al-Ni-Si and Al-Ni-Ge systems[15]. The highest σ_f value for the metal-metalloid type amorphous alloys is 450 MPa which is higher than that for the fcc solution in Al-Ni-Si system, but the strength level is considerably

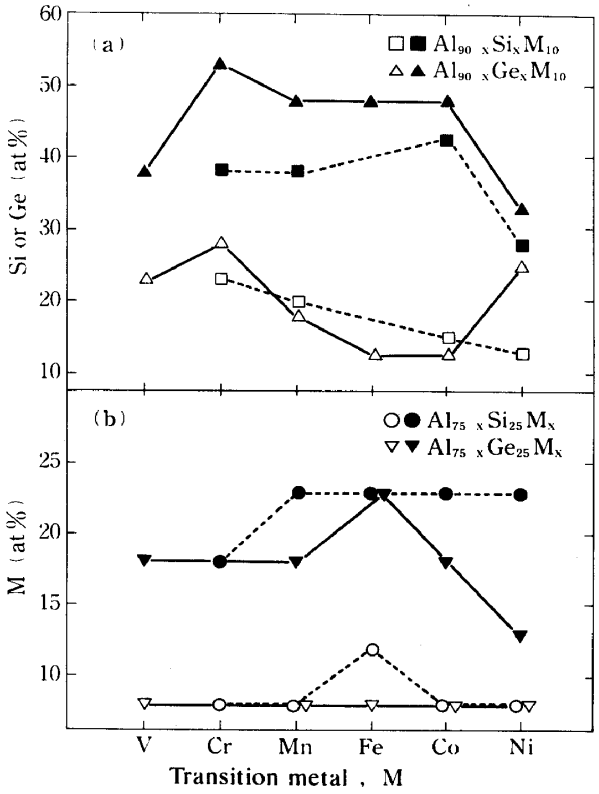

Fig. 7 Compositional ranges for formation of an amorphous phase in melt-spun Al-Si-M and Al-Ge-M (M=V, Cr, Mn, Fe, Co or Ni) ternary alloys. The open and solid marks represent the lower and upper limits of each composition range, respectively.

lower than that of the fcc solution in Al-Ce-Fe system. Considering that the metalloids of Si and Ge have a repulsive interaction against Al, the strengthening of Al-based amorphous alloys seems to be rather difficult in the metal-metalloid system.

On the other hand, one can list up Al-Ln binary[9] and Al-Ln-M[10,11] and Al-EM-LM[18] ternary systems as the metal-metal type amorphous alloys. The EM in the Al-EM-LM system is Ti, Zr, Hf, V, Nb, Ta, Cr, Mo or W and the LM represents Mn, Fe, Co, Ni or Cu. Although the amorphous phase in the Al-EM-LM system is obtained in the solute range of about 12 to 50 at%, the amorphous phase is not formed in all the alloy systems and is limited to the alloy systems of Al-Zr-Fe, Al-Zr-Co and Al-Zr-Ni etc. where the binary alloys consisting of EM and LM can be amorphized. The amorphous phase in these alloy systems has good bending ductility in the composition range above about 80 at% Al and the σ_f exhibits relatively high values of 600 to 800 MPa.

Although the alloy system in which a high tensile strength above 980 MPa (100 kg/mm^2) is obtained in Al-based amorphous alloys is

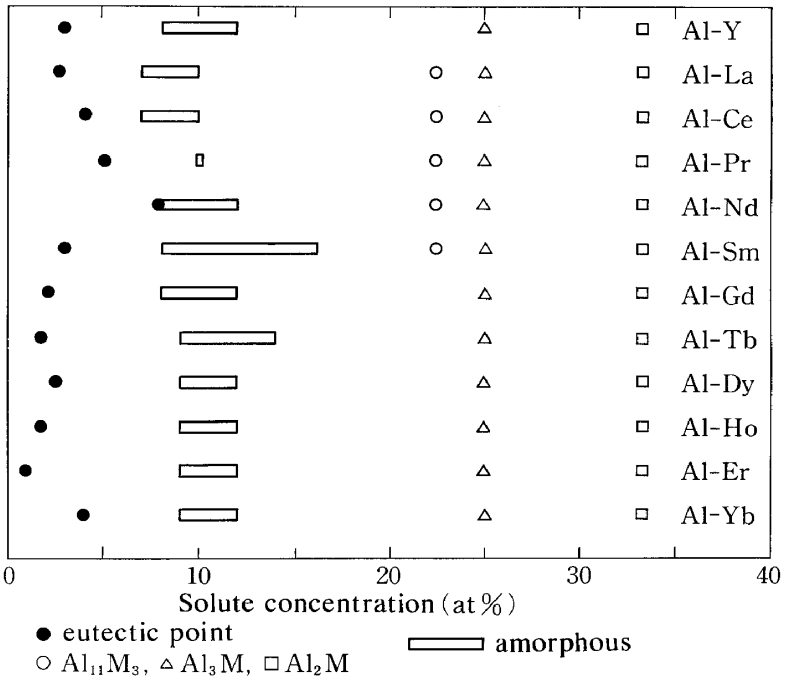

Fig. 8 Relation between the composition ranges for formation of an amorphous phase in melt-spun Al-Ln binary alloys and the eutectic and compound compositions of Al-Ln alloys.

limited to the Al-Ln-M ternary system[19], the data on Al-Ln binary amorphous alloys will be presented first because the binary system is regarded to be a fundamental system for the high-strength ternary amorphous alloys. As shown in Fig. 8, the amorphous phase in Al-Ln binary system is formed in the range 7 to 13 at% Ln[9]. In addition, eutectic points and the compositions of intermetallic compounds in the equilibrium binary alloys are also shown for reference. The formation range of the amorphous phase is located in an intermediate range between eutectic point and stoichiometric intermetallic compound where the temperature interval between the onset and offset points of slidification is as wide as 305 to 627 K. Thus, the formation of the amorphous phase in the Al-Ln system is not explained by the lowering of T_m and the atomic size ratio between Al and Ln atoms. That is, the glass formation is thought to originate from the rise of T_g resulting from a steep increase of vscosity of the supercooled liquid with decreasing temperature. The steeply increased viscosity seems to come from the development of a short-range ordering of Al-Ln pairs resulting from the large negative interaction between Al and Ln atoms.

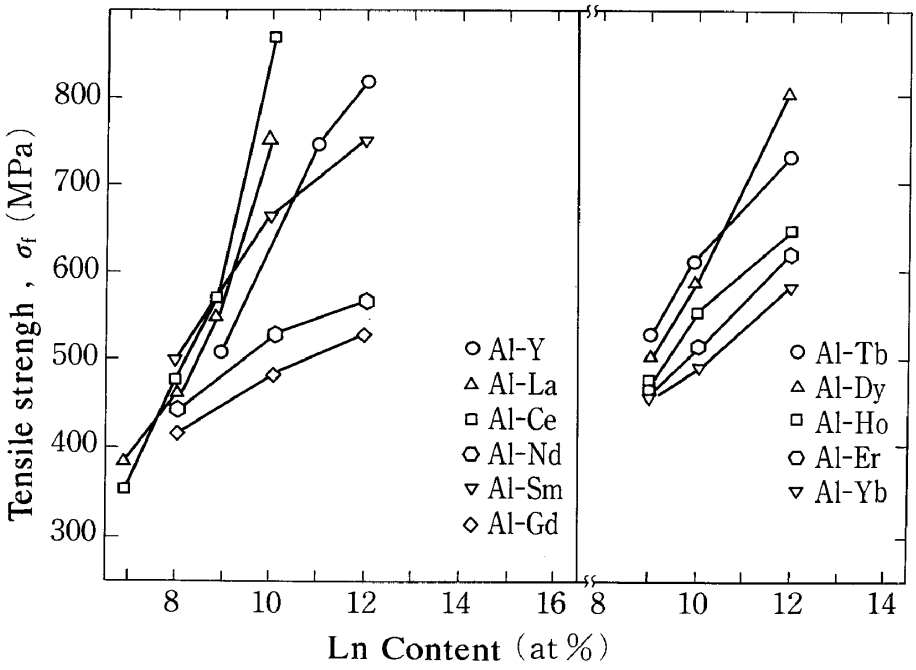

Fig. 9 Change in the tensile fracture strength (σ_f) as a function of Ln content for amorphous Al-Ln binary alloys.

Figure 9 shows the change in σ_f of the Al-Ln amorphous alloys with Ln content[9]. The σ_f increases from 350 to 900 MPa with increasing Ln content.

In order to obtain an Al-based amorphous alloy with further improved mechanical strengths, the effect of M elements on the formation range, strength and thermal stability of Al-based amorphous alloys was examined for Al-Ln-M ternary alloys. As shown in Fig. 10[10], the glass formation is significantly extended by the addition of the M elements such as Fe, Co, Ni and Cu and the addition of Ni is the most effective. The addition of these M elements is also effective for the increase in T_x from about 500 to 800 K as well as the enhancement of σ_f, H_v and Young's modulus (E). As shown in Table 2[19], the σ_f of Al-Y-Ni and Al-La-Ni amorphous alloys is above 1000 MPa and the highest value reaches as high as 1140 MPa. In addition, the E and H_v are in the range of 70 to 90 GPa and 260 to 350, respectively. It is thus notable that the σ_f and H_v of their amorphous alloys are about twice as high as the highest values of conventional crystalline Al-based alloys. Most recently, the σ_f has been reported[20] to increase to 1280 MPa for an Al-Y-Ni-Co system. Subsequent progress in an optimization of alloy component is highly

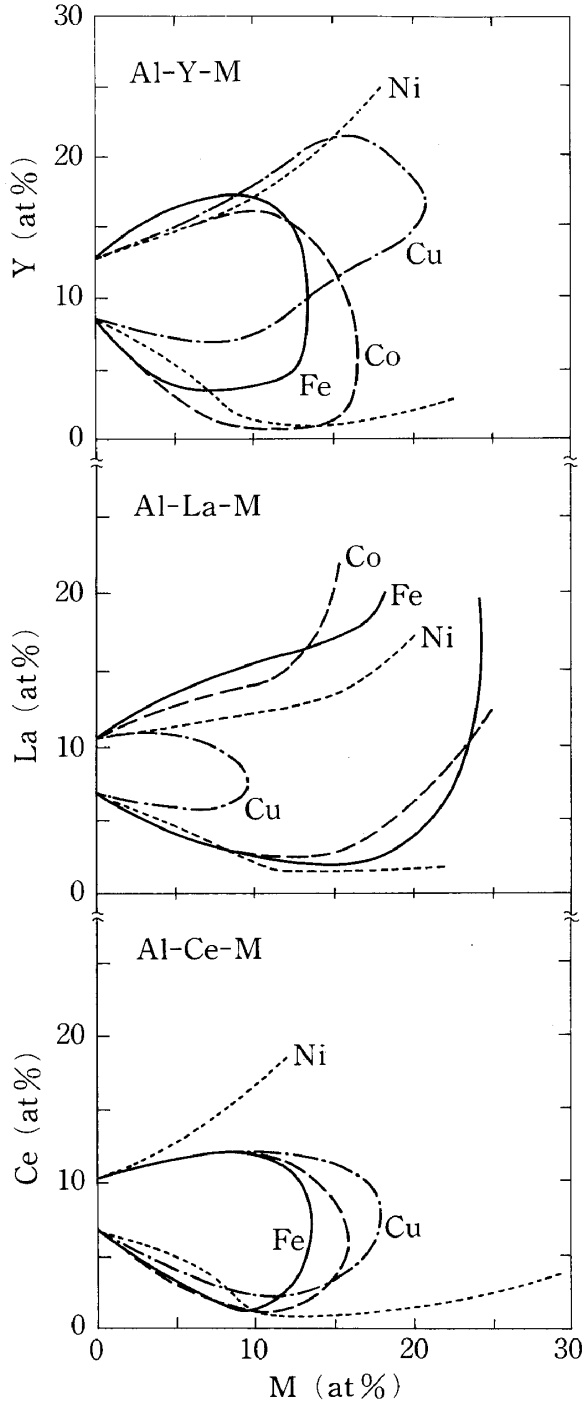

Fig. 10 Composition ranges for formation of an amorphous single phase in melt-spun Al-Y-M, Al-La-M and Al-Ce-M alloys.

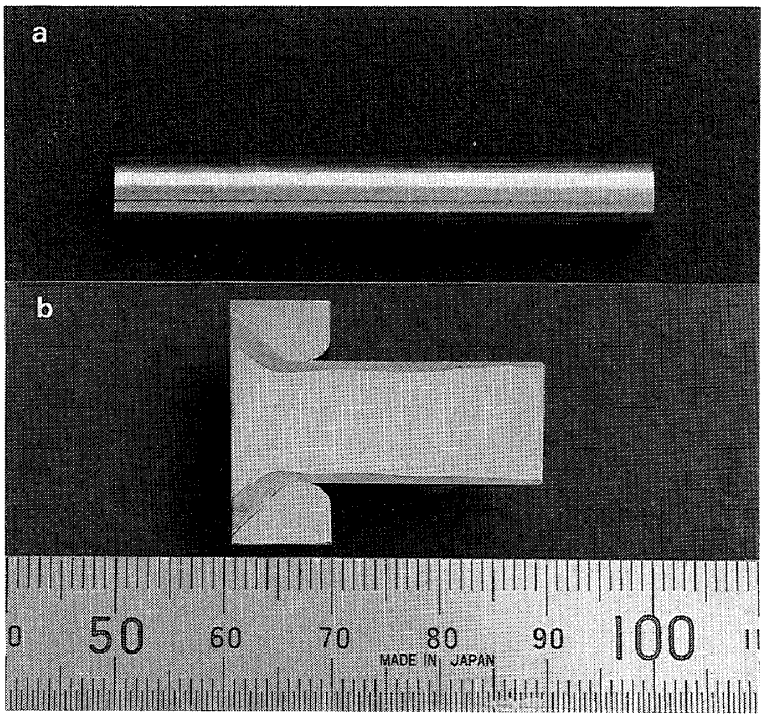

Fig. 11 Photographs of external appearance (a) and longitudinal cross section (b) of an $Al_{85}Y_{10}Ni_5$ bulk material produced by extrusion at 543 K of the amorphous Al-Y-Ni powder which was filled up into pure Cu tube.

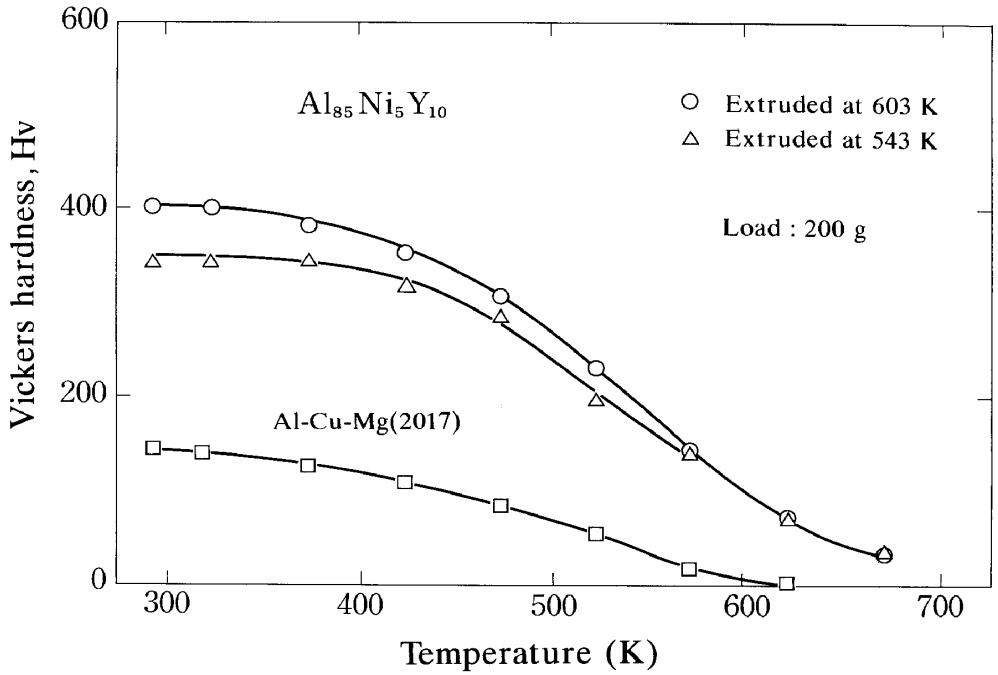

Fig. 12 Temperature dependence of Vickers hardness (H_v) for an amorphous $Al_{85}Y_{10}Ni_5$ bulk. The data of the commercial Al-Cu-Mg duralumin alloy (2017) are also shown for comparison.

Table 2 Mechanical properties of aluminum-based amorphous alloys.

Alloy (at%)	σ_f (MPa)	E (GPa)	H_v	$\varepsilon_{t,f}=\sigma_f/E$	$\varepsilon_{c,y}\cong 9.8H_v/3E$
$Al_{88}Y_2Ni_{10}$	920	71.0	340	0.013	0.016
$Al_{87}Y_8Ni_5$	1140	71.2	300	0.016	0.014
$Al_{87}La_8Ni_5$	1080	88.9	260	0.012	0.010
$Al_{84}La_6Ni_{10}$	1010	83.6	280	0.012	0.011
$Al_{86}Ce_4Ni_{10}$	810	54.6	300	0.015	0.018
$Al_{85}Ce_5Ni_{10}$	935	59.4	320	0.016	0.018

$\varepsilon_{t,f}$ and $\varepsilon_{c,y}$ represent tensile fracture strain and compressive yield strain, respectively.

expected to bring about an Al-based amorphous alloy with higher mechnaical strengths. Furthermore, it is important to point out that the corrosion resistance in NaOH and HCl solutions for the Al-based amorphous alloys is better by about 70 to 230 times, respectively, than that for conventional high-strength crystalline Al-Cu-Mg alloy (2024)[21].

The reason for the high mechanical strengths of the Al-Ln-M amorphous alloys can be explained by the same concept as that for the fcc Al-Ce-Fe solution. That is, there is a strong attractive interaction between Al and Ln or M atoms and the amorphous structure has a developed short-range ordering among these atoms. The development of the short-range ordered structure is thought to be the origin for appearance of the high mechanical strengths. This concept is also supported from the results of X-ray structure analyses[22] and electronic properties[23] obtained for Al-Y and Al-Y-Ni amorphous alloys.

VI. Formability of Amorphous Alloy Powders into a Bulk Form and Mechanical Strengths of their Bulk Materials

The reason why the Al-based amorphous alloys have attracted great attention is due to the appearance of the glass transition and supercooled liquid region in the temperature range below crystallization temperature (T_x)[24]. The appearance of the supercooled liquid region implies a possibility of consolidation of the amorphous ribbon or powder into a bulk form in the supercooled liquid region even for the high-strength amorphous alloys. By

extruding Al-Y-Ni amorphous powders produced by high-pressure gas atomization[25] at temperatures near T_g, we succeeded in producing bulk materials with a high density above 99 % consisting mainly of an amorphous phase, as shown in Fig. 11. Furthermore, these bulk materials exhibit high heat-resistant hardness values above 200 in the temperature range below 550 K as shown in Fig. 12 as well as compressive strength of about 1500 MPa, tensile strength of 900 to 1000 MPa, Young's modulus of about 135 GPa and H_v of about 420[26]. These data allow us to conclude that the Al-based bulks are high strength materials with high specific tensile strength, high specific Young's modulus and high heat-resistant strength. Although the extrusion ratio for these bulk materials is as low as 4 to 8, it is noticed that the bulk materials have high mechanical strengths. This is presumably because the good viscous flowability in the supercooled liquid region causes the formation of highly dense bulk materials. It is thus notable that the Al-based amorphous alloys have a good deformability resulting from the existence of the supercooled liquid region and a good deformability as well as the high mechanical strengths. These features are unique characteristics which cannot be obtained for the Al-based fcc supersaturated solutions.

VII. Conclusion

Our recent data on the formation and mechanical strengths of supersaturated fcc and amorphous alloys in Al-based alloy systems have been reviewed in the viewpoint that the amorphous phase is also a kind of solution saturated with solute elements. These supersaturated solid solutions have been clarified to exhibit high mechanical strengths in a static stress condition. However, in order to develop further these Al-based alloys as practical materials, it is necessary to establish an extrusion technique to produce a large-scale consolidated material and to accumulate the data on the dynamic strengths and environmental embrittlement of the consolidated materials. Anyhow, a trial to utilize the high mechanical strengths of the Al-Ln-M supersaturated solutions produced by rapid solidification has just started in spite of the long history of development for Al-based alloys and hence a subsequent progress as a new type of high specific strength material is expected. It has been clarified[27] that these supersaturated solid solutions decompose to crystalline mixed phases upon subsequent heating, leading to a secondary hardening. Since the origin for the secondary hardening is

due to fine dispersion particles and is different from that for the soild solution hardening, the data on the mixed phases were omitted in this review.

References

(1) W. Klement, R.H. Willens and P. Duwez, Nature, 187 (1960), 869.

(2) C. Suryanarayana, Rapidly Quenched Metals, A Bibliography, 1973-1979, Plenum, New York, (1980).

(3) T.R. Anantharaman, P. Ramachandrarao, C. Suryanarayana, S. Lele and K. Chattopadhyay, Trans. Ind. Inst. Metals, 30 (1978), 423.

(4) Materials Science of Amorphous Metals, ed. T. Masumoto, Ohmu Pub. Co., Tokyo (1982).

(5) H. Jones, Aluminum, 54 (1978), 274.

(6) M. Watanabe, Y. Izumi, H.M. Kimura, A. Inoue and T. Masumoto, private communication, (1989).

(7) A. Inoue, K. Ohtera and T. Masumoto, Jpn. J. Appl. Phys., 27 (1988), L736.

(8) A. Inoue, K. Ohtera, T. Zhang, K. Kita and T. Masumoto, Jpn. J. Appl. Phys., 27 (1988), L1583.

(9) A. Inoue, T. Zhang, K. Kita and T. Masumoto, Trans. Japan Inst. Metals, 30 (1989), 870.

(10) A. Inoue, K. Ohtera, A.P. Tsai and T. Masumoto, Jpn. J. Appl. Phys., 27 (1988), L280.

(11) A. Inoue, K. Ohtera, A.P. Tsai and T. Masumoto, Jpn. J. Appl. Phys., 27 (1988), L736.

(12) A. Inoue, H. Yamaguchi, M. Kikuchi and T. Masumoto, 6th Non-Ferrous Met. Symposium, eds. I. Nagy and G. Konczos, Hungarian Academy Sciences, (1989), p.148.

(13) Powder and Powder Metallurgy of Aluminum Alloys, ed. Technical Research Society of Aluminum Powder and Powder Metallurgy, (1989).

(14) H. Horimura, M. Kikuchi, A. Inoue and T. Masumoto, private communication, (1988).

(15) A. Inoue, M. Yamamoto, H.M. Kimura and T. Masumoto, J. Mater. Sci. Lett., 6 (1987), 194.

(16) A. Inoue and T. Masumoto, Bulletin Japan Inst. Metals, 28 (1989), 968.

(17) A. Inoue, Y. Bizen, H.M. Kimura, T. Masumoto and M. Sakamoto, J. Mater. Sci., 23 (1988), 3640.

(18) A.P. Tsai, A. Inoue and T. Masumoto, Met. Trans., 19A (1988),

1369.

(19) A. Inoue, K. Ohtera, A.P. Tsai and T. Masumoto, Jpn. J. Appl. Phys., 27 (1988), L479.

(20) A. Inoue, N. Matsumoto and T. Masumoto, Mater. Trans., JIM, 31 (1990), 493.

(21) A. Inoue, K. Ohtera and T. Masumoto, Proc. MRS Int. Meeting on Advanced Materials, Vol.3, ed. M. Doyama et al., MRS, Pittsburgh, (1989), p.251.

(22) E. Matsubara, Y. Waseda, A. Inoue, K. Ohtera and T. Masumoto, Z. Naturforsch., 44a (1989), 814.

(23) M. Pont, J. Gonzalo, K.V. Rao and A. Inoue, Phys. Rev. B, 40 (1989), 1345.

(24) A. Inoue, K. Ohtera, A.P. Tsai, H.M. Kimura and T. Masumoto, Jpn. J. Appl. Phys., 27 (1988), L1579.

(25) A. Inoue, K. Kita, K. Ohtera, H.M. Kimura and T. Masumoto, J. Mater. Sci. Lett., 7 (1988), 1287.

(26) A. Inoue, T. Masumoto, K. Ohtera and K. Kita, Proc. First Japan Int. SAMPE Symposium on New Materials and Processes for the Future, ed. M. Igata et al., Nikkan Kogyo Shimbun Ltd., Tokyo, (1989), p.7.

(27) A. Inoue, H. Yamaguchi, M. Kikuchi and T. Masumoto, Sci. Rep. Res. Inst. Tohoku Univ., 35A (1990), 101.